Journal of Biomedical Materials Research Part B, Applied Biomaterials 70B, p.146-151, 2004

Quantitative analysis of biological specimens by X-ray scanning analytical microscopy.

Motohiro UO, Masaya TANAKA and Fumio WATARI

Dental Materials and Engineering, Department of Oral Health Science, Graduate School of Dental Medicine, Hokkaido University

*** Address of corresponding author:**

Motohiro Uo

Dental Materials and Engineering, Department of Oral Health Science, Graduate School of Dental Medicine, Hokkaido University

North 13 West 7, Kita-ku, Sapporo, 060, JAPAN

Telephone & Facsimile:+81-11-706-4251 E-mail: uo@den.hokudai.ac.jp

Abstract

X-ray scanning analytical microscopy (XSAM) can be used to visualize the elemental distribution in biological specimens. In this study, the authors prepared standard specimens for XSAM and performed quantitative analysis of various elements dissolved in soft tissues. Two different types of standard specimens were prepared. Methylmethacrylate (MMA) resin-based standard specimens were prepared with organic compounds of elements for low-concentration standards and lithium borate glass-based standard specimens were prepared with oxides of elements for higher concentration standards. Using these standard specimens, the P and Ca concentrations in normal rat tissue and dissolved Ni, Fe and Ni concentrations around metal implanted tissues were quantitatively analyzed. The estimated concentrations of dissolved Fe, Cu and Ni from the implants were 1000, 40 and 20mM, respectively. From the concentration levels causing inflammation around these implants, the high toxicity for soft tissue of Ni and Cu at low concentrations, e.g., 10mM was confirmed. The toxicity of Cu was estimated as next to that of Ni. In contrast, Fe had low toxicity in spite of high concentrations of dissolved Fe of as much as 1000mM. In this study, it was possible to estimate the non-metallic elements and low-concentration metallic elements dispersed in soft tissue by XSAM.

Keywords: X-ray scanning analytical microscopy (XSAM), quantitative analysis, standard specimen, dissolution, implant, elemental mapping,

Introduction

X-ray scanning analytical microscopy (XSAM) enables elemental distribution analysis for Na to U by energy dispersive spectroscopy of fluorescent X-rays in air without pretreatment even if the sample contains water[1]. This feature is desirable for the analysis of biological specimens[2-5]. The authors have reported application of XSAM for soft tissue analysis[2-4]. The authors also reported the rapid analysis of metallic dental restoratives[6]. XSAM was useful for visualization of the dissolution and distribution of highly toxic and chemically unstable metal implants in soft tissue. It clearly revealed the dissolved region around pure nickel in soft tissue and showed that it was in good agreement with the highly inflammated tissue region. There is, however, a limitation in that the obtained information is qualitative to semi-quantitative. To evaluate dissolved metallic elements in soft tissue, it is necessary to establish concentration standards for each element. The preparation of MMA resin-based standard specimens for various elements has been reported[7]. In a previous report [5], the authors prepared Ni standard specimens with nickel acetylacetonate dispersed in methylmethacrylate (MMA) resin and evaluated the Ni dissolution content in soft tissue.

In this report, MMA-based and borate glass-based standard specimens of P, S, Ca, Cr, Mn, Fe, Ni, Cu and Zn were prepared and subjected to quantitative analysis by XSAM of various elements dissolved in soft tissue.

Experimental procedure

(1) Preparation of standards with MMA resin matrix

The resin standards for P, S, Ca, Cr, Mn, Fe, Ni, Cu and Zn were prepared using the organometallic compounds listed in Table 1. Each chemical was dissolved in methylmethacrylate (MMA) to obtain appropriate concentrations and polymerized at 60^{o}C. For the resin standard, Ca was dissolved $CaCl_2$ in hydroxyethylmethacrylate (HEMA) and mixed with MMA. Each element was concentrated by the contraction in the polymerization process of MMA. The contraction of MMA in was reported to be 21.2%. Therefore, the concentration of each standard was estimated considering with the MMA contraction. The polymerized standards were sliced 1mm thick and observed by XSAM under the same conditions as implanted specimens.

(2) Preparation of standard specimens with borate glass matrix

The high concentration standard was prepared with lithium borate glass. Various amounts of Fe_2O_3, Cu_2O and $Ca(OH)_2$ were mixed into 10wt%Li_2O-B_2O_3 glass. The mixture was melted at 1000^{o}C for 2 hours in air using an alumina crucible and poured onto a brass plate. The poured melt was quenched by pressing with another brass plate to obtain a glassy solid 1mm thick. The cooled glass was crushed into small pieces. The pieces of standards were set on an acryl plate and analyzed with XSAM.

(3) XSAM observation of standard specimens and metal-implanted soft tissue

XSAM observation was carried with the incident X-rays generated from a Rh anode under conditions of 50kV and 1mA. X-ray irradiation was done using an X-ray guide tube (XGT) 100mmϕ in diameter. The stage scanning was repeated in air 100 times for about three days, and the mapping image was integrated. The average X-ray intensity from the standard specimens was estimated from the average brightness of the mapping image.

The implant materials consisted of 99.9% Cu, 99.9% Ni and 99.5% Fe wires (1mmϕ×10mm). The procedure of implantation and preparation of specimens was described elsewhere [3]. The resin-embedded tissue blocks were sliced 1mm thick, polished with alumina emulsion and emloyed for XSAM observation. Calibration curves of Kα peak intensity and the concentration of each element were made using standards.

Results

Figure1 shows the Mn, Zn and Cr mapping images of resin-based standard specimens. The brightness of Mn and Cr standards increased with the concentration. The relationship between the fluorescence X-ray intensity and the brightness is provided by the contrast bar at the bottom of photograph. From the brightness of each standard specimen and the contrast bar, the calibration curve could be estimated.

The estimated calibration curves are shown in Figs. 2, 3 and 4. Figure 2 shows the relationship between the fluorescent X-ray intensities of P, S and Ca and their concentrations in an MMA matrix. The concentration range of Ca standard was restricted to low concentration due to the quite low solubilities less than 3mM of calcium chloride in HEMA. The X-ray intensity of S slightly increased with increase in the S concentration. That of P showed a nonlinear increase with regard to the P concentration. It was considered to be due to the self absorption of fluorescent X-rays by P itself.

Figure 3 shows the relationships between the fluorescent X-ray intensities of the metallic elements (Cr, Mn, Fe, Ni, Cu and Zn) and their concentrations in the MMA matrix. The concentration ranges of Cu and Zn were restricted to low concentrations due to the quite low solubilities less than 1mM of copper acetylacetonate and bis(2,4-pentanedionato) zinc in MMA. For four other elements, Cr, Mn, Fe and Ni, their organic compounds showed relatively good solubility in MMA and linear relationships between the fluorescent X-ray intensities and their concentrations in an MMA matrix were obtained.

Figure 4 shows the relationships between the fluorescent X-ray intensities of Ca, Fe and Cu and their concentrations in the lithium borate glass matrix as the high-concentration standards. Each specimen was transparent and no crystallization was observed. This indicated that the lithium borate glass showed the high solubility of Ca, Fe and Cu oxide and high-concentration standards were successfully prepared. Linear relationships were observed for Ca, Cu and the low concentration range of Fe. In the high concentration range of Fe, a nonlinear relationship was observed. It was considered to be due to the self absorption of fluorescent X-rays by Fe itself.

Figure 5 shows the Ca distribution in the rat subcutaneous layer and the estimated concentration using the Ca standard specimen. The Ca concentration in the rat subcutaneous tissue is higher than the range of resin based Ca standard (Fig.3), therefore, the borate glass-based Ca standard (Fig.4) was used for the estimation. The highest Ca concentration in the rat subcutaneous tissue was estimated to be 60mM at the muscle layer.

Figure 6 shows the elemental distribution around the Fe, Cu and Ni implants by XSAM elemental mapping. The implants were placed in the center of observed areas. Clear dissolution of the metallic element was observed around the implants in the mapping images. Figure 7 shows the line analysis of Cu, Ni and Fe mapping images shown in Fig. 6 using the standards of Ni (Fig. 3) and Cu and Fe (Fig. 4). Fe had an extremely high concentration around the implant, estimated to be 1000mM. The maximum concentrations of Cu and Ni were estimated to be 40mM and 20mM, respectively.

Discussion

In this study, the standards for XSAM were prepared using organo-metallic compounds dissolved in MMA resin and metal oxides dissolved in lithium borate glass. The tissue specimens were embedded in MMA. Therefore, the MMA-based standard was desirable. However, the species and concentration ranges of standards were limited because of the low solubility of metal organic compounds in MMA. Therefore, standard specimens with wider concentration ranges were prepared using a glass matrix. A glass matrix usually has wide solubility for various metallic oxides. For the use of the XSAM standard, low X-ray absorption is required. The lithium borate matrix consisted of light element cations and low absorption was expected. The mass absorption coefficient of 10wt%Li_2O-B_2O_3 glass was estimated to be 36(cm^2/g) for the X-ray of 6.4keV from the mass absorption rate of the contained elements[8] This coefficient is higher than that of MMA resin (14 cm^2/g) but much lower than SiO_2(77 cm^2/g), which is the base component of ordinary glass. Therefore, lithium borate glass was considered an appropriate matrix for the XSAM standard. Figures 2,3 and 4 show the relationships between the fluorescent X-ray intensities of elements and their concentrations in MMA and glass-based matrices. The increment of the X-ray intensity for the concentration of each element shows the XSAM sensitivity of the element. As shown in Fig. 9, the sensitivity increased with the atomic number of element. This tendency means that XSAM shows higher sensitivity for heavier elements.

The authors reported that the Ca, P and S distribution in rat soft tissue could be visualized using XSAM [4]. Using the results in Fig. 2, the P concentration in the rat skin could be estimated as approximately10mM (0.03wt%). The S and Ca concentrations in soft tissue were outside of the range of the MMA-based standard specimens. In a previous report [2], the authors could estimate the concentration of dissolved Ni in rat soft tissue from implanted Ni. However, the other elements, e.g., dissolved Cu and Fe in the soft tissue from these implants and Ca in rat soft tissue, were outside of the range of the MMA-based standards. Therefore, borate glass-based standards with high contents of the elements were developed and the concentrations in soft tissue could be estimated as shown in Fig. 5 and Fig. 7. In Fig. 5, the estimated Ca concentration in the rat muscle is approximately 60mM (0.2wt%). The Ca concentration is reported to be typically 0.006wt% in rat skeletal muscle. The estimated Ca concentration in present study was more than ten times higher than the reported value. Shrinkage during specimen preparation and MMA resin condensation would be one reason for this difference.

The dissolution of metallic elements from pure metal implants was also estimated as shown in Fig. 7. Fe showed a much higher concentration around the implant, estimated as 1000mM, than Cu and Ni. Figure 8 shows histological tissue images with low magnification around the implants in the area shown in Fig. 7. Severe tissue degradation was observed around Cu and Ni implants, whereas relatively moderate tissue damage was observed around the Fe implant. In a previous report [3], severe inflammatory responses such as necrosis of cells, emigration of macrophages and dilation of blood vessels were observed around the Ni and Cu implants in histological observation at high magnification. The Cu implant was encapsulated in a cystic structure and the inside of the cystic structure was filled with a blue-colored exudate. The exudate was lost during specimen processing. Therefore, the original

concentration of Cu was considered to be higher than the present concentration. Considering the severe inflammatory response around the Ni implant and the rather low dissolved concentration, the high toxicity of Ni for soft tissue was confirmed. The toxicity of Cu was estimated to be less than that of Ni but both showed high toxicity even at a low concentration such as 10mM. In contrast, Fe was not as toxic as Ni and Cu even at the high concentration of 1000mM.

Conclusions

For XSAM quantitative analysis of various elements dissolved in soft tissues, two different types of standard specimens, MMA-based and borate glass based, were prepared for P, S, Ca, Cr, Mn, Fe, Ni, Cu and Zn. The solubility of metal organic compounds in MMA was very low. Therefore, the low concentration standard specimens were made with the MMA base. In contrast, the borate glass matrix usually has wide solubility for various metallic oxides and the standard specimens for higher concentrations were made with the glass base. Using these standard specimens, the P and Ca concentrations in rat normal tissue and dissolved Ni, Fe and Ni concentrations in metal-implanted tissues were quantitatively analyzed. The estimated concentrations of dissolved Fe, Cu and Ni were 1000, 40 and 20mM, respectively. From the concentration level that caused inflammation around the implants, the high toxicity of Ni for soft tissue was confirmed. The toxicity of Cu was estimated as slightly less than that of Ni. In contrast, Fe showed low toxicity in spite of a concentration of dissolved Fe as high as 1000mM.

In this study, various standard specimens were developed for soft tissue analysis by XSAM and it was possible to quantitatively analyze various elements dispersed in soft tissue. In particular, the metallic element with low concentrations could be quantitated by XSAM and the relationship between the concentration and tissue reaction estimated.

Acknowledgements

The work was supported by the Hokkaido Foundation for The Promotion of Scientific and Industrial Technology. Part of this work was also supported by Research on Advanced Medical Technology in Health and Labour Sciences Research Grants from the Ministry of Health, Labour and Welfare of Japan.

References

1 Hosokawa, Y., Ozawa, S., Nakazawa, H.and Nakayama, Y., An X-ray guide tube and a desk-top scanning X-ray analytical microscope. *X-Ray Spectrom*.,1997, **26**, 380-387.

2 Uo, M., Watari, F., Yokoyama, A., Matsuno, H. and Kawasaki, T., Dissolution of nickel and tissue response observed by X-ray scanning analytical microscope. *Biomaterials*, 1999, **20**, 747-755

3 Uo, M., Watari, F., Yokoyama, A., Matsuno, H. and Kawasaki, T. Tissue reaction around metal implants observed by X-ray scanning analytical microscopy. *Biomaterials*, 2001, **22**, 677-685

4 Uo, M., Watari, F., Yokoyama, A., Matsuno, H. and Kawasaki, T. Visualization and detectability of elements rarely contained in soft tissue by X-ray scanning analytical microscopy and electron-probe micro analysis. *Biomaterials*, 2001, **22**, 1787-1794

5 Xu, S., Kitajo, H., Kawashima, I., Yamane, Y., Murata, M., Shibata, T., Arisue, M., Endo, K., Shi, S., Ohno, H. X-ray scanning analytical microscopic and scanning electron microscopic studies of an unusual case of dens invaginatus. *Higashi Nippon Dental Journal*, 2000, **19**, 143-157

6 Uo, M., Watari, F. Rapid analysis of analysis of metallic dental restoratives using X-ray scanning analytical microscopy. Submitted for publication in *Dental Materials*

7 Roomans, G.M. and Van Gaal, H.L.M., Organometallic and organometalloid compounds as standards for microprobe analysis of epoxy resin embedded tissue. *J. Microscopy*, 1977, **109**, 235-240

8 Weast, R.C. ed., CRC handbook of chemistry and physics 69th edition, CRC Press Inc., Florida, 1988-1989, p.E144-147

Figure captions

Fig. 1 XSAM mapping images of Mn, Zn and Cr standard specimens.

Fig. 2 Relationships between the fluorescent X-ray intensities of P, S and Ca and their concentrations in MMA resin matrix.

Fig. 3 Relationships between the fluorescent X-ray intensities of Cr, Mn, Fe, Ni, Cu and Zn and their concentration in MMA matrix.

Fig. 4 Relationships between the fluorescent X-ray intensities of Ca, Fe and Cu and their concentrations in lithium borate glass matrix.

Fig. 5 The Ca distribution image of rat soft tissue and estimated Ca concentration in line analysis.

Fig. 6 The elemental distribution image around the Fe, Ni and Cu implants in rat soft tissue.

Fig. 7 The dissolved Fe, Ni and Cu concentration curves around implants. (along the white line shown in Fig. 6)

Fig. 8 Histological images of the Fe-, Ni- and Cu-implanted tissues.

Fig. 9 The experimentally obtained dependence of fluorescent X-ray sensitivity on the atomic number.

Table 1 Organometallic compounds used for standard specimens

Element	Compound
P	Tryphenylphosphine*
S	Sodium N,N-Diethyldithiocarbamate Tryhydrate*
Ca	Calcium chloride*
Cr	Tris (2,4-pentanedionato) chromium (III)**
Mn	Tris (2,4-pentanedionato) manganese(III)**
Fe	Dycyclopentadienyliron(II)*
Ni	Nickel(II) acetylacetonate, Dyhydrate*
Cu	Copper(II) acetylacetonate*
Zn	Bis (2,4-pentanedionato) zinc(II)**

* Kanto Kagaku (Tokyo, Japan) ** Dojindo (Kumamoto, Japan)

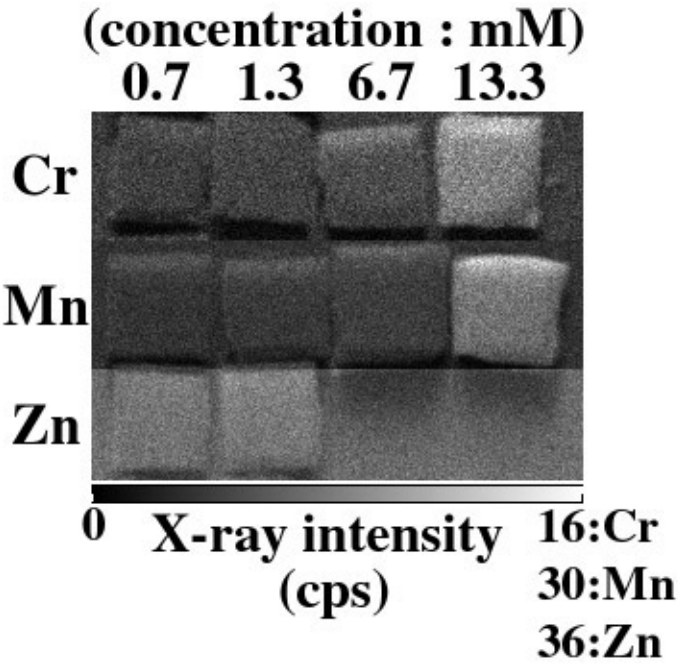
(concentration : mM)
0.7
1.3
6.7
13.3
Cr
Mn
Zn
0
X-ray intensity
(cps)
16:Cr
30:Mn
36:Zn

Fig. 1

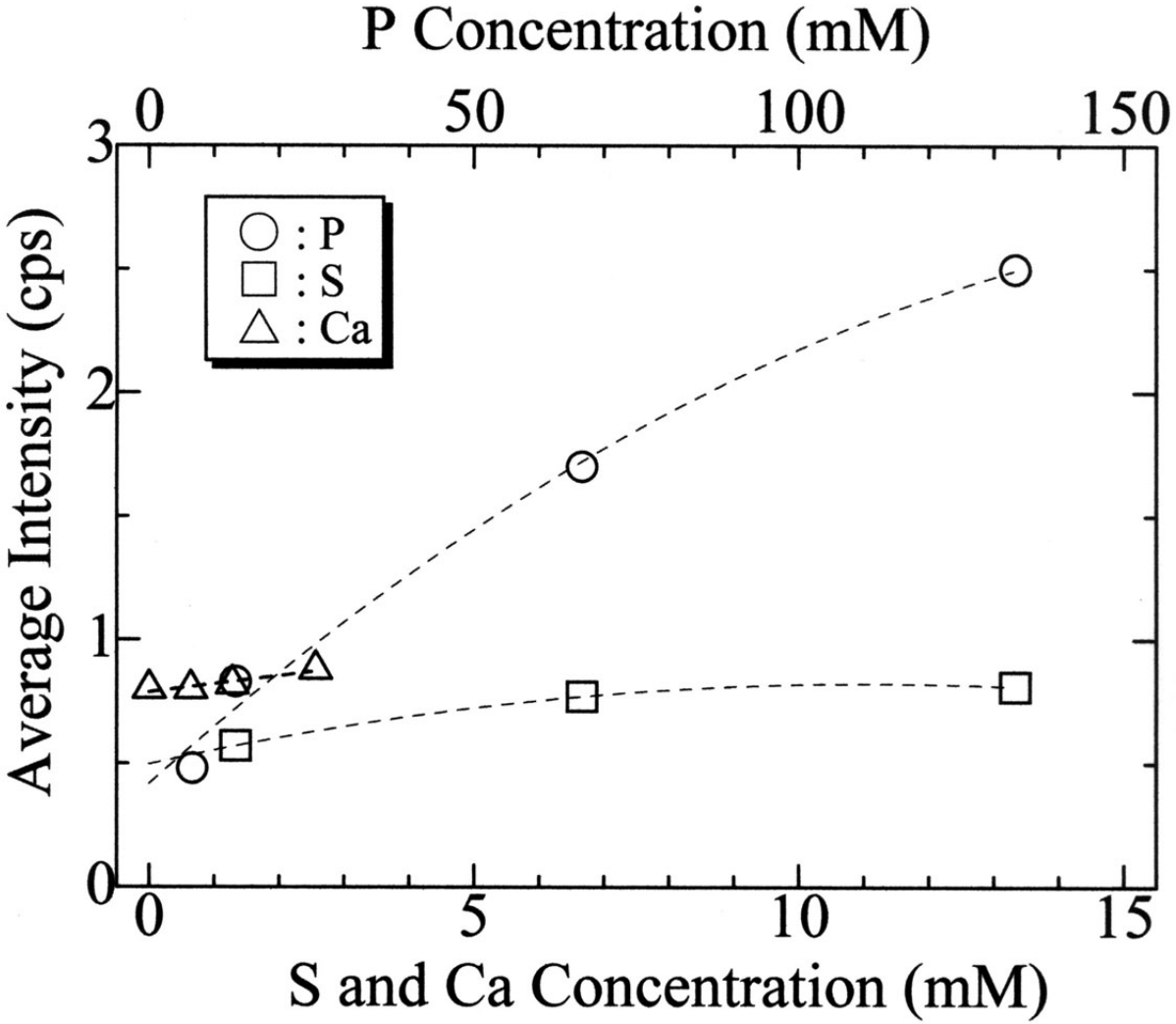
P Concentration (mM)
0
50
100
150
3
2
1
0
Average Intensity (cps)
○ : P
□ : S
△ : Ca
0
5
10
15
S and Ca Concentration (mM)

Fig.2

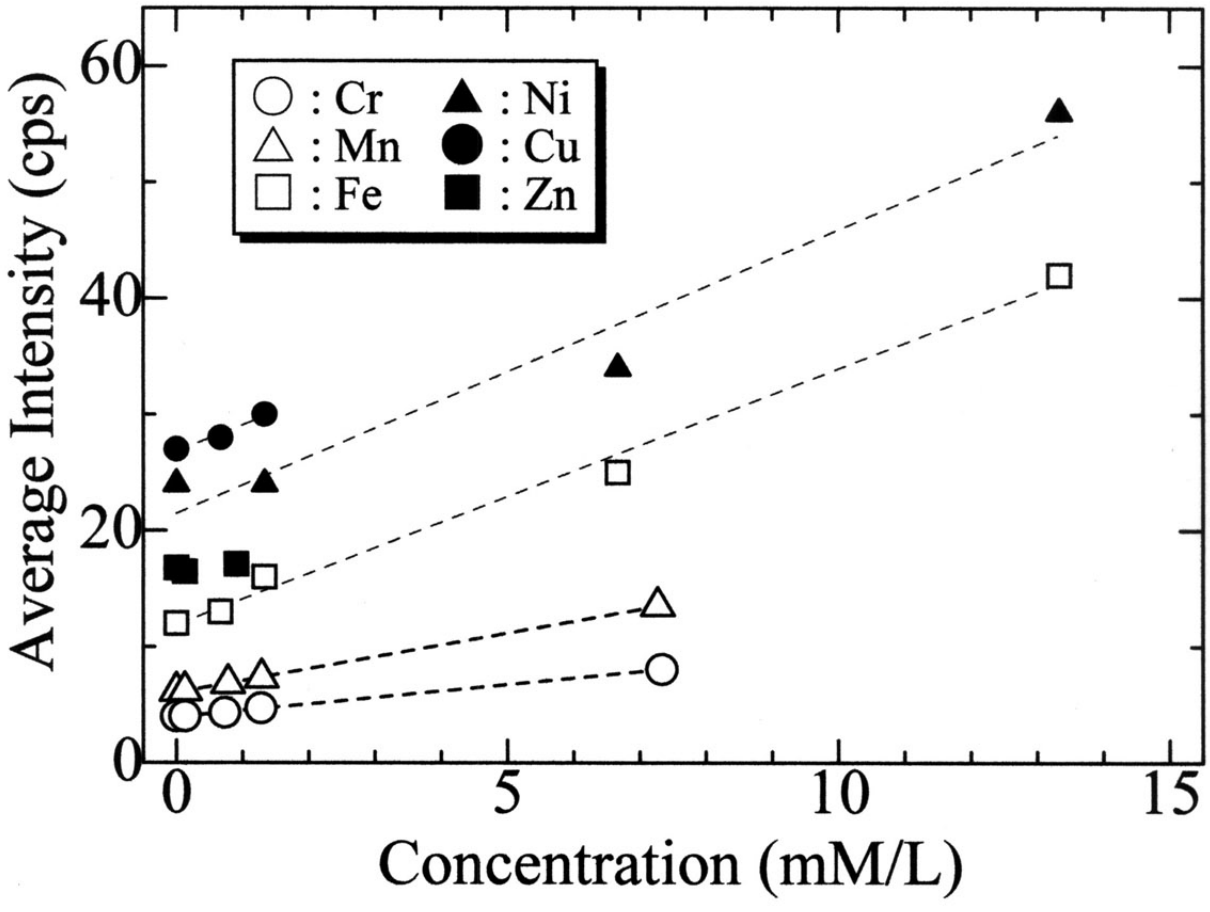
○ : Cr
△ : Mn
□ : Fe
▲ : Ni
● : Cu
■ : Zn
Average Intensity (cps)
0
20
40
60
0
5
10
15
Concentration (mM/L)

Fig.3

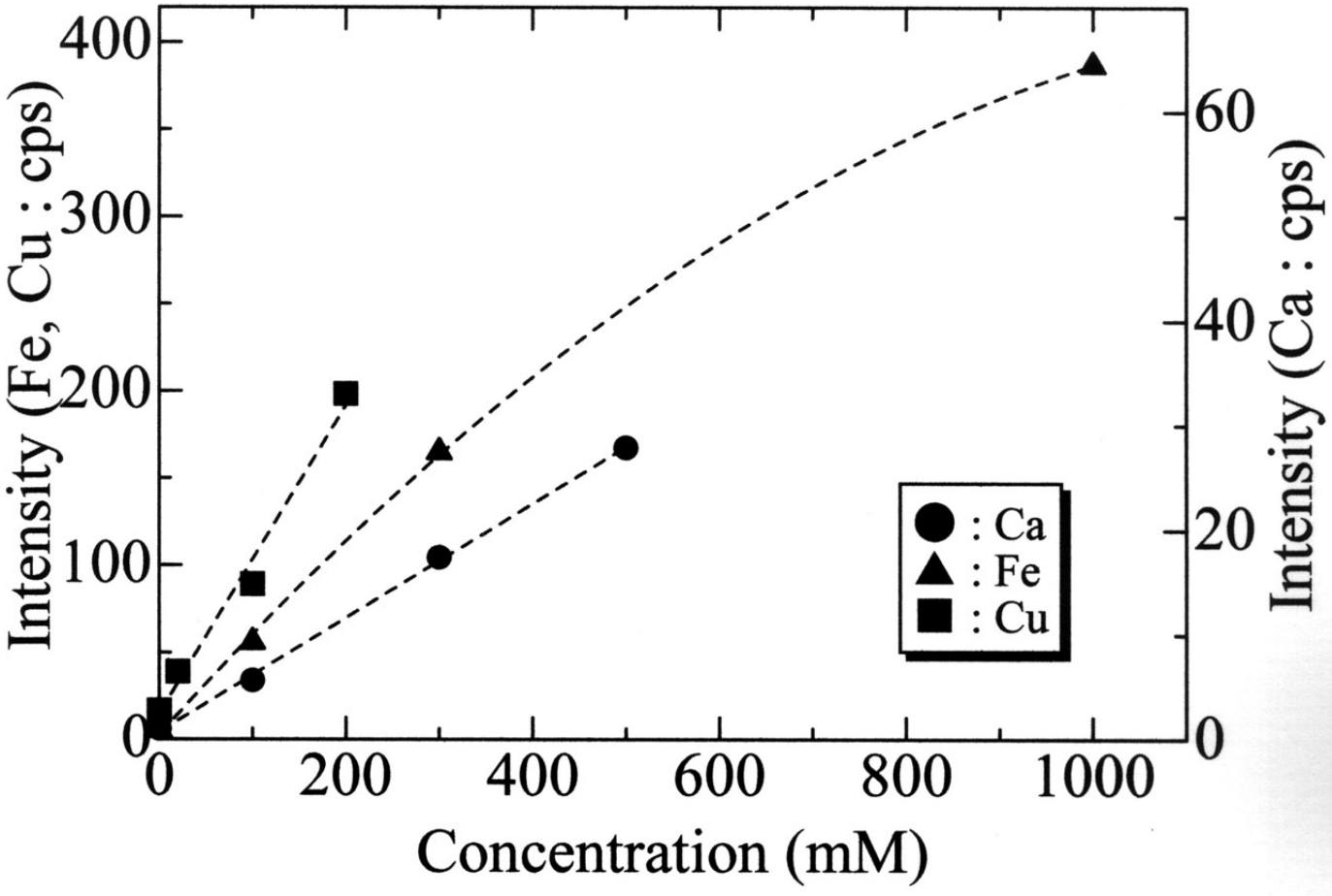
Intensity (Fe, Cu : cps)
Intensity (Ca : cps)
Concentration (mM)
0
100
200
300
400
0
20
40
60
0
200
400
600
800
1000
: Ca
: Fe
: Cu

Fig.4

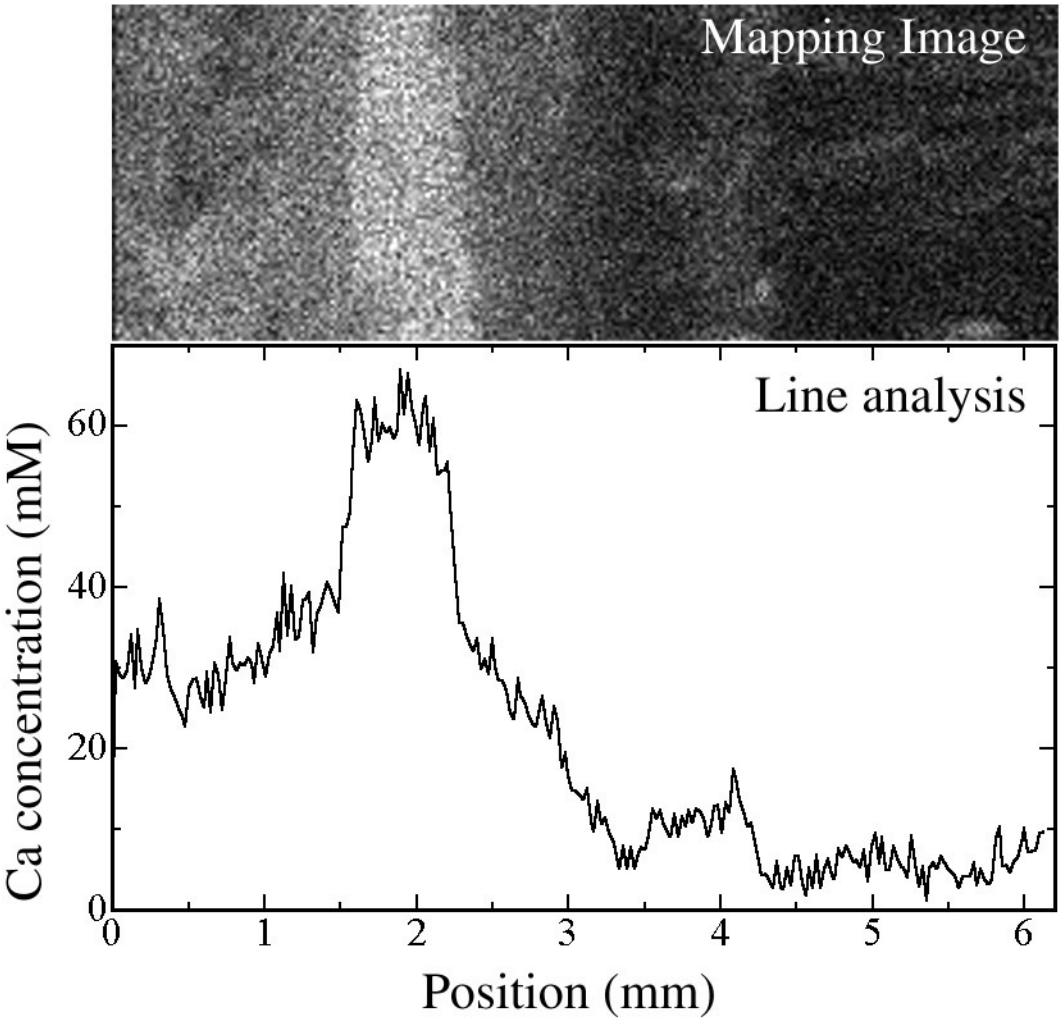
Mapping Image
Line analysis
Ca concentration (mM)
0
20
40
60
0
1
2
3
4
5
6
Position (mm)

Fig.5

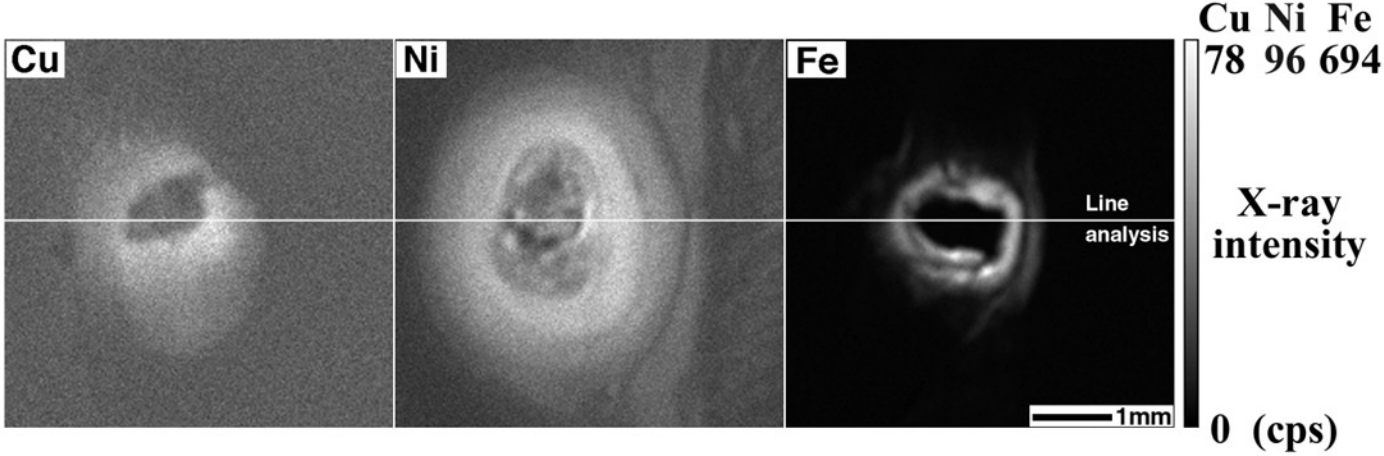
Cu
Ni
Fe
Line
analysis
1mm
Cu Ni Fe
78 96 694
X-ray
intensity
0 (cps)

Fig.6

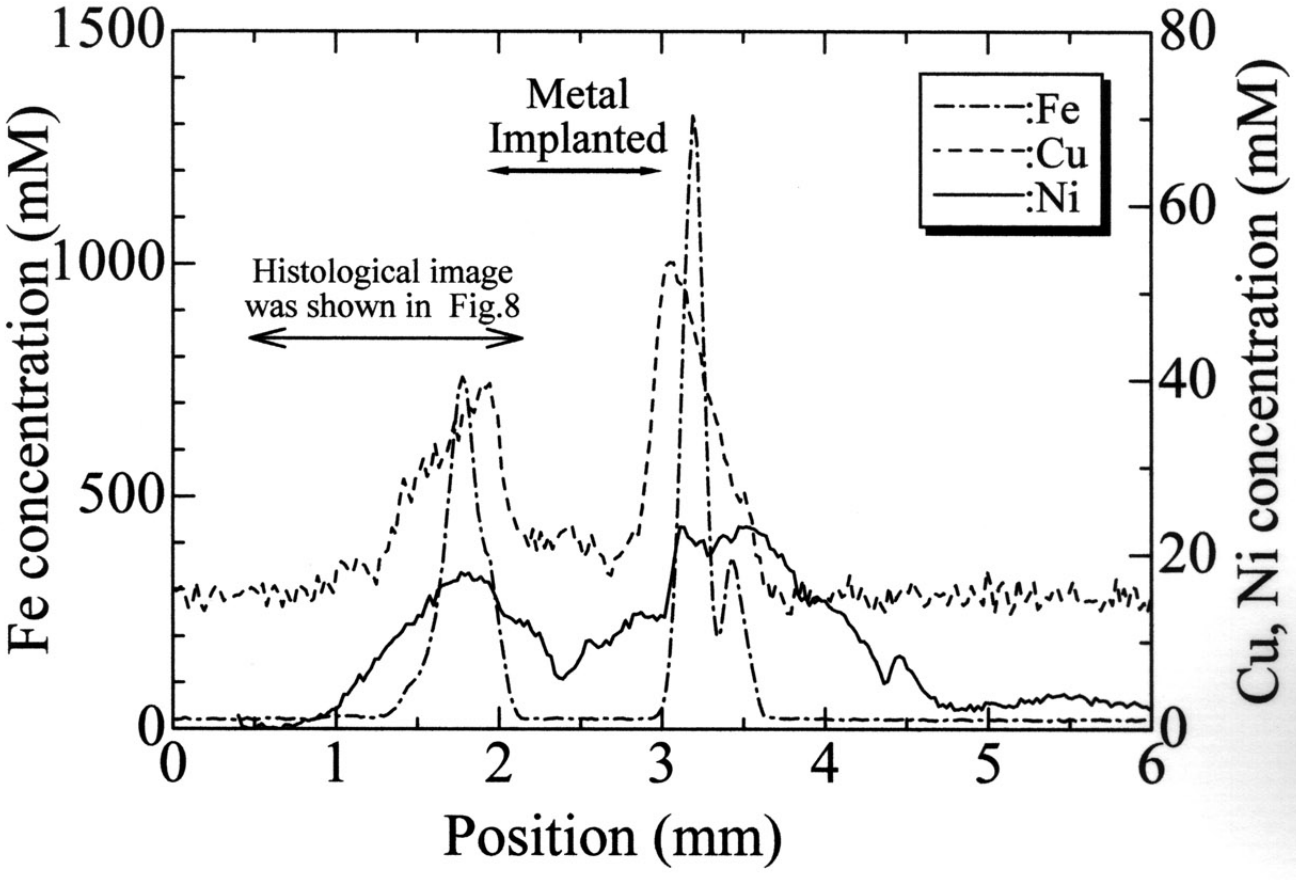
1500
1000
500
0
80
60
40
20
0
Fe concentration (mM)
Cu, Ni concentration (mM)
Metal
Implanted
Histological image
was shown in Fig.8
:Fe
:Cu
:Ni
0
1
2
3
4
5
6
Position (mm)

Fig.7

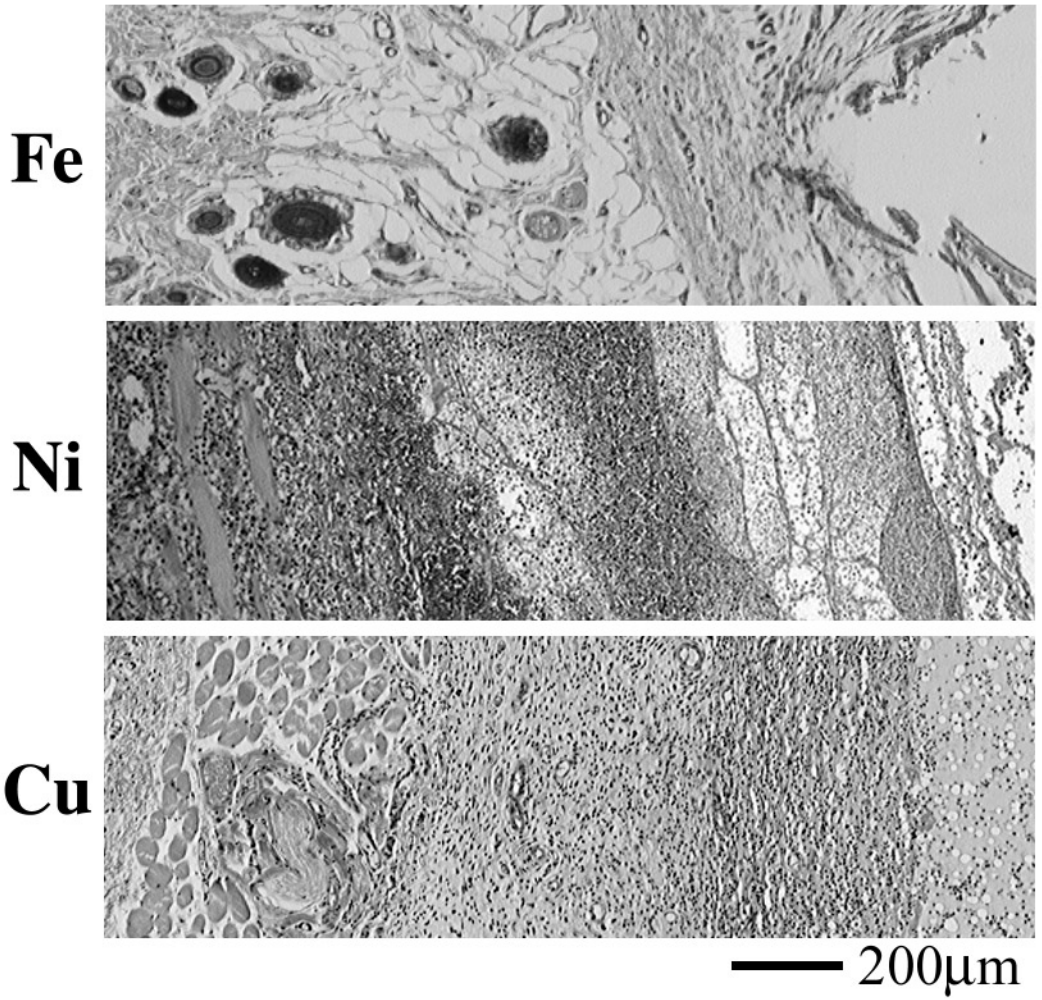

Fig.8

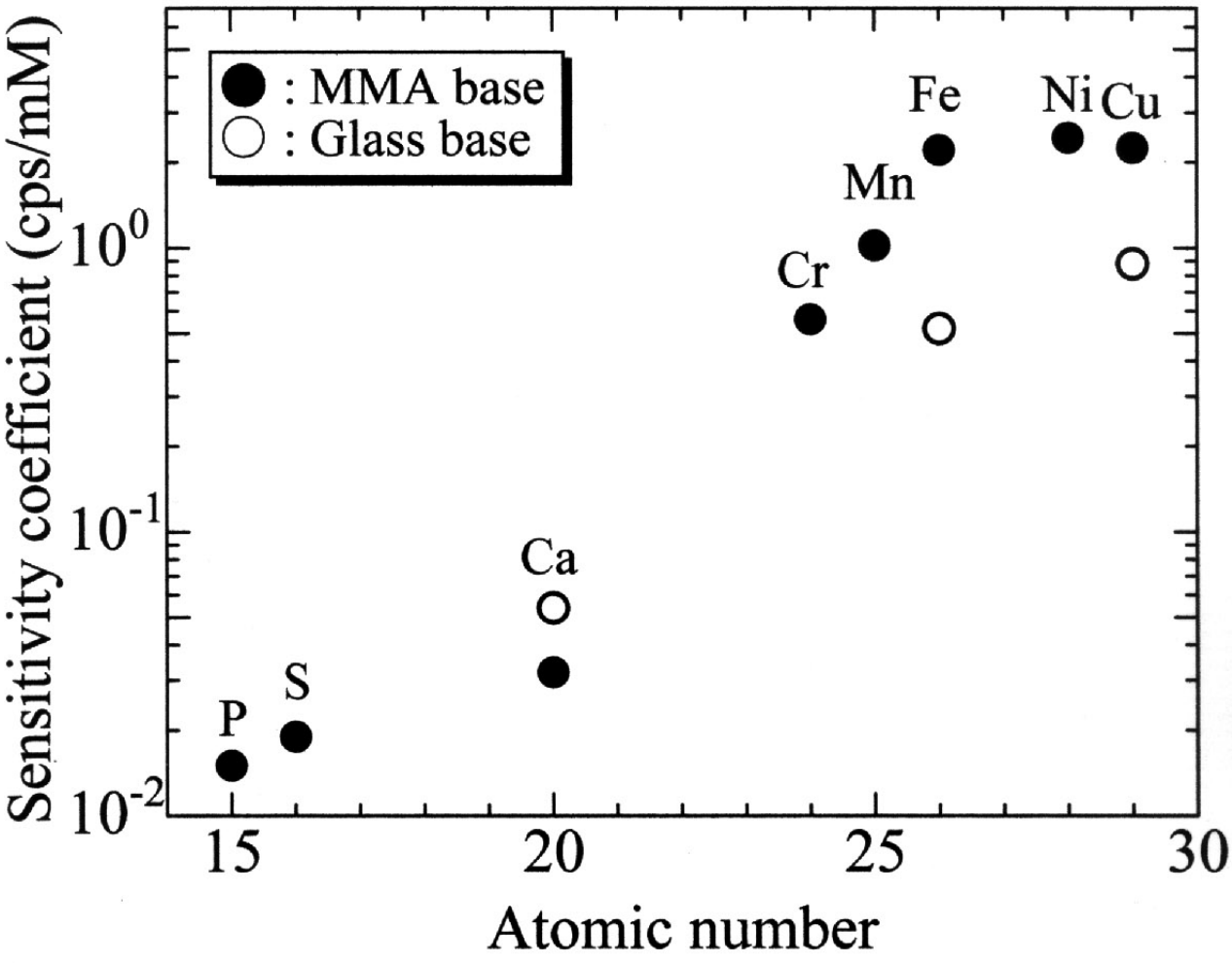
● : MMA base
○ : Glass base
Sensitivity coefficient (cps/mM)
10^0
10^{-1}
10^{-2}
P
S
Ca
Cr
Mn
Fe
Ni
Cu
15
20
25
30
Atomic number

Fig.9